Application of the CYNUS code for multigroup MSR problem calculation

Michał Kurowski, Muhammad Wazif Mohd Sallehhudin, Jooil Yoon*

KEPCO International Nuclear Graduate School, 658-91 Haemaji-ro, Seosaeng-myeon, Ulju-gun, Ulsan 45014, Republic of Korea
*Corresponding author: jiyoon@kings.ac.kr

***Keywords :** Coarse Mesh Finite Difference, Nodal Expansion Method, Source Expansion Nodal Method, cylindrical geometry, molten salt reactor

1. Introduction

Growing interest in 4th generation nuclear reactor designs requires reliable and robust reactor physics numerical codes to assure and prove safe operation under postulated accident scenarios. Among the most promising designs are Molten Salt Reactors (MSR) and High-Temperature Gas-cooled Reactors (HTR), whose native coordinate system is cylindrical rather than Cartesian. Considering this fact, establishment of an efficient, reliable and accurate neutronics code that is based in the cylindrical coordinate system is desired, and significant academic effort has been already devoted in pursuit of this goal [1, 2, 3, 4].

General and preferable approach for this problem is two-step calculation procedure. Where a high-fidelity Monte Carlo solver is used to generate homogenized few-group cross sections and equivalence parameters, which then form the basis for the whole-core diffusion based deterministic calculations.

In this paper, the development of a CYNUS code, that is direction-specific diffusion neutronic solver for cylindrical geometry based on two-node kernels, is discussed. Additionally, it is validated against 3D IAEA "cylindricalized" LWR benchmark [5], and utilized to solve a proposed multigroup MSR problem.

Numerical routine for the one-node kernel approach has already been developed and shown to provide satisfactory accuracy [6]. However, this work proposes and incorporates alternative two-node kernel approach.

a. Two-node kernel approach is implemented as it features higher numerical stability than its one-node alternative. Additionally, node-sweeping process is not needed to establish converged nodal neutron currents between adjacent nodes, which may improve the computation time.

b. Source Expansion Nodal Method is based on the analytical solution of the transverse-integrated neutron diffusion equation, where the source term is approximated as a fourth-order polynomial expansion. By utilizing this numerical scheme, nodal neutron currents converge for a coarser mesh size than in the regular NEM approach [7].

2. Numerical procedure

2.1 Cylindrical FDM formulation

A general framework for the Finite Difference Method (FDM) in the cylindrical coordinate system had to be derived as a foundation for the CMFD numerical scheme. The basic formulation of the 3D steady-state neutron diffusion equation with energy discretization in cylindrical coordinate system given is given as (1).

$$\begin{aligned} &-D_g\nabla^2\phi_g(r,\theta,z)+\Sigma_{t,g}\phi_g(r,\theta,z)= \\ &=\frac{\chi_g}{k_{eff}}\psi(r,\theta,z)+S_g(r,\theta,z) \end{aligned} \tag{1}$$

$$\psi(r,\theta,z)=\sum_{g'=1}^{G}(\nu\Sigma_f)_{g'}\phi_{g'}(r,\theta,z) \tag{2}$$

$$S_g(r,\theta,z)=\sum_{g'=1}^{G}\Sigma_{s,g'\to g}\phi_{g'}(r,\theta,z) \tag{3}$$

After integration over volume of the node (denoted by superscript k), than dividing by it, and applying divergence theorem to the leakage term, the equation takes following form (4).

$$\begin{aligned} &\frac{-D_g^k}{V^k}\oiint_{S^k}\nabla\phi_g^k(r,\theta,z)\cdot d\vec{S}+\Sigma_{t,g}\bar{\phi}_g^k= \\ &=\frac{\chi_g}{k_{eff}}\bar{\psi}(r,\theta,z)+\bar{S}_g(r,\theta,z) \end{aligned} \tag{4}$$

The discrete node's volume is bounded by six surfaces that are orthogonal to each other from cylindrical coordinate system point of view. Therefore, the surface integral can be also expressed as a summation of the neutron currents multiplied by their corresponding surface areas (8). Gradient of the neutron flux is approximated by linear interpolation, derived on the basis of neutron flux and current continuity, between adjacent nodes (5).

$$J_g^{k,u\pm}=-\tilde{D}_g^{k,u\pm}\left(\phi_g^R-\phi_g^L\right) \tag{5}$$

$$I_g^{k,u\pm}=J_g^{k,u\pm}A^{k,u\pm} \tag{6}$$

$$\tilde{D}_g^{k,u\pm}=\frac{2\beta_g^R\beta_g^L}{\beta_g^R+\beta_g^L},\qquad \beta_g=\frac{D_g}{h} \tag{7}$$

$$\begin{aligned} &\frac{1}{V^k}\sum_{u=r,\theta,z}\left(I_g^{k,u+}-I_g^{k,u-}\right)+\Sigma_{t,g}^k\bar{\phi}_g^k= \\ &=\frac{\chi_g^k}{k_{eff}}\bar{\psi}^k+\bar{S}_g^k \end{aligned} \tag{8}$$

Where $u\pm$ represents the surface oriented in the direction u, that is located on the right (+) or left (-) side of the node. L and R superscripts represent the left and right adjacent nodes to given surface, respectively. h represents the distance between the centers of adjacent nodes, and A is the surface area.

Beyond this point, calculation procedure was similar to the Cartesian geometry case, as the set of equations, after

rearrangement, was reduced to an eigenvalue problem (9), which was solved using the power iteration method.

$$\mathbf{M}\vec{\phi} = \frac{1}{k}\mathbf{F}\vec{\phi} \tag{9}$$

2.2 Cylindrical two-node kernel CMFD

CMFD is a well-established numerical routine used for solving the deterministic eigenvalue neutron diffusion problems. It offers an exceptionally accurate numerical solution for coarse mesh size, by incorporating the neutron diffusion correction factor (10). It is based on the nodal neutron current, and is applied in alternative formulation of the neutron current (11).

$$\hat{D}_g^{k,u\pm} = \frac{J_{g,FDM}^{k,u\pm} - J_{g,NEM}^{k,u\pm}}{\bar{\phi}_g^R + \bar{\phi}_g^L} \tag{10}$$

$$J_{g,CMFD}^{k,u\pm} = -\tilde{D}_g^{k,u\pm}(\bar{\phi}_g^R - \bar{\phi}_g^L) - \hat{D}_g^{k,u\pm}(\bar{\phi}_g^R + \bar{\phi}_g^L) \tag{11}$$

2.3 Transverse integration procedure

In order to establish the nodal neutron current, the neutron diffusion equation has been transverse-integrated, to decouple the 3D partial differential equation into three 1D ordinary differential equations. It is obtained by integration over two directions, leaving out direction of interest dependency. This results in an additional term in the equation, the transverse leakage, that accommodates for leakage in the directions orthogonal to the direction of interest. In the Cartesian geometry all three equations are expressed in the same way.

However, because of the Laplace operator formulation in cylindrical coordinate system (12), the transverse integration procedure yields a set of three different equations.

$$\nabla^2\phi = \frac{1}{r}\frac{\partial}{\partial r}\left(r\frac{\partial\phi}{\partial r}\right) + \frac{1}{r^2}\frac{\partial^2\phi}{\partial\theta^2} + \frac{\partial^2\phi}{\partial z^2} \tag{12}$$

It is worth noting that the azimuthal direction is inherently coupled with the radial direction, which significantly complicates the transverse integration procedure. To resolve this issue, a constant radius approximation (13), has been incorporated [6].

$$\frac{1}{r^2}\frac{\partial^2\phi}{\partial\theta^2} \approx \frac{1}{r_k^2}\frac{\partial^2\phi}{\partial\theta^2} \tag{13}$$

After incorporating the following approximation, the azimuthal and axial directions behave in the same way as in the Cartesian geometry. Therefore, the variables have been normalized following $\xi_u = \frac{2(u-u_k)}{\Delta u_k}$ to make Legendre polynomials applicable as basis functions for the neutron flux expansion.

$$Q_{gu}^k(u) = \frac{\chi_g^k}{k_{eff}}\psi_u^k(u) + S_{gu}^k(u) - L_{gu}^k(u) \tag{14}$$

$$-\frac{D_g^k}{r}\frac{d}{dr}\left(r\frac{d\phi_{gr}^k(r)}{dr}\right) + \Sigma_{t,g}^k\phi_{gr}^k(r) = Q_{gr}^k(r) \tag{15}$$

$$-\frac{4D_g^k}{r_k^2\Delta\theta_k^2}\frac{d^2\phi_{g\theta}^k(\xi_\theta)}{d\xi_\theta^2} + \Sigma_{t,g}^k\phi_{g\theta}^k(\xi_\theta) = Q_{g\theta}^k(\xi_\theta) \tag{16}$$

$$-\frac{4D_g^k}{\Delta z_k^2}\frac{d^2\phi_{gz}^k(\xi_z)}{d\xi_z^2} + \Sigma_{t,g}^k\phi_{gz}^k(\xi_z) = Q_{gz}^k(\xi_z) \tag{17}$$

2.4 Nodal neutron current

Once the transverse integrated neutron diffusion equations have been established, the neutron flux expansion was determined with an appropriate nodal method. Afterwards, the nodal neutron current was calculated following its direct definition.

$$J_{gu}^k(u) = -D_g^k\frac{d\phi_{gu}^k(u)}{du} \tag{18}$$

2.5 Source Expansion Nodal Method

SENM offers high accuracy in the neutron current approximation [7]. Two-node SENM has been applied to the azimuthal and axial directions. Where the neutron flux expansion is based on Legendre polynomials P_i and hyperbolic trigonometric functions.

$$\begin{aligned}\phi_{gu}^k(\xi_u) &= A_g^k\sinh(\kappa_g^k\xi_u) + \\ &+ B_g^k\cosh(\kappa_g^k\xi_u) + \sum_{i=0}^{4} c_{gi}^k P_i(\xi_u)\end{aligned} \tag{19}$$

2.6 Nodal Expansion Method

NEM has been applied alternatively in the radial direction, as the SENM method is not suitable. Moreover, since the usual neutron flux expansion based on Legendre polynomials fails to account for the Jacobian present during integration, an alternative set of basis functions has been applied [8].

$$P_1^k(r) = 6\frac{r-r_k}{\Delta r_k} - \frac{\Delta r_k}{2r_k} \tag{20}$$

$$P_2^k(r) = 12\left(\frac{r-r_k}{\Delta r_k}\right)^2 - 1 \tag{21}$$

$$P_3^k(r) = \left(2\frac{r-r_k}{\Delta r_k} - \frac{\Delta r_k}{10r_k}\right)\left(1 - 4\left[\frac{r-r_k}{\Delta r_k}\right]^2\right) \tag{22}$$

$$P_4^k(r) = 80\left(\frac{r-r_k}{\Delta r_k}\right)^4 - 24\left(\frac{r-r_k}{\Delta r_k}\right)^2 + 1 \tag{23}$$

The following basis functions P_i^k share the property that their constant term equals to the average neutron flux of k-th node.

$$\bar{\phi}_g^k = \frac{1}{r_k\Delta r_k}\int_{r_k-\frac{\Delta r_k}{2}}^{r_k+\frac{\Delta r_k}{2}} \phi_{gr}^k(r)rdr = a_{g0}^k \tag{24}$$

As the average neutron flux value is provided by the previous CMFD iterations, there are in total four unknown neutron flux expansion coefficients per node.

$$\phi_{gr}^k(r) = \bar{\phi}_g^k + \sum_{i=1}^{4} a_{gi}^k P_i^k(r) \tag{25}$$

2.7 Transverse leakage expansion coefficients derivation

Transverse leakage function in the radial direction was set to be a second order polynomial built upon the same basis functions. Expansion coefficients were obtained on basis of the average transverse leakage assigned to node of interest and its neighbors in radial direction (27). Where $m = L, k, R$.

$$L_g^k(r) = \sum_{i=0}^{2} l_{gi}^k P_i^k(r) \tag{26}$$

$$\frac{1}{r_m \Delta r_m} \int_{r_m - \frac{\Delta r_m}{2}}^{r_m + \frac{\Delta r_m}{2}} L_g^k(r) r dr = \bar{L}_g^m \tag{27}$$

Based on the property (24) of basis functions, the constant term was shown to be equal to average transverse leakage of k-th node.

$$\bar{L}_g^k = \frac{1}{r_k \Delta r_k} \int_{r_k - \frac{\Delta r_k}{2}}^{r_k + \frac{\Delta r_k}{2}} L_g^k(r) r dr = l_{g0}^k \tag{28}$$

Based on condition (27), for left and right neighboring nodes, set of equations has been constructed and other two transverse leakage expansion coefficients were calculated.

2.8 Radial flux expansion coefficients derivation

In order to calculate nodal neutron current passing through each radially oriented surface, flux expansion coefficients had to derived. In this work three types of surfaces have been recognized, each requiring a specific approach.

2.9 Inner surfaces

For each inner surface regular two-node NEM has been applied. Where expansion coefficients were given by a linear system of eight equations. These were based on neutron flux and current continuity conditions at common surface, as well as first three moments of the Galerkin weighted residual method. Inner surfaces are defined to be located between two adjacent nodes, and none of them contains the center of the cylindrical coordinate system at $r = 0$.

First two equations require the neutron flux and current to be continuous at the common surface between two adjacent nodes. Based on this requirement and the previously established neutron flux expansion formula, following equations have been derived. Where $\beta_g = \frac{D_g}{\Delta r}$.

- Neutron flux continuity condition

$$\phi_{gr+}^L = \phi_{gr-}^R \tag{29}$$

$$\begin{aligned} &a_{g1}^L (3 - \frac{\Delta r_L}{2r_L}) + 2a_{g2}^L + a_{g1}^R (3 + \frac{\Delta r_R}{2r_R}) - 2a_{g2}^R = \\ &= \bar{\phi}_{gr-}^R - \bar{\phi}_{gr+}^L \end{aligned} \tag{30}$$

- Neutron current continuity condition

$$J_{gr+}^k = J_{gr-}^{k+1} \tag{31}$$

$$-D_g^k \frac{d\phi_{gr+}^k}{dr} = -D_g^{k+1} \frac{d\phi_{gr-}^{k+1}}{dr} \tag{32}$$

$$\begin{aligned} &6a_{g1}^L \beta_g^L + 12a_{g2}^L \beta_g^L + a_{g3}^L (\frac{2D_g^L}{5r_L} - 4\beta_g^L) + \\ &+ 16a_{g4}^L \beta_g^L - 6a_{g1}^R \beta_g^R + 12a_{g2}^R \beta_g^R + \\ &+ a_{g3}^R (\frac{2D_g^R}{5r_R} + 4\beta_g^R) + 16a_{g4}^R \beta_g^R = 0 \end{aligned} \tag{33}$$

Next, the first three moments of the Galerkin weighted residual method has been applied per each node $m = L, R$. Where zeroth moment is equivalent to nodal balance equation (8), with the only difference being the r-direction neutron leakage is based on the neutron flux expansion, following relation (18).

$$R_{gr}^k(r) = -\frac{D_g^k}{r} \frac{d}{dr} \left(r \frac{d\phi_{gr}^k(r)}{dr} \right) + \Sigma_{t,g}^k \phi_{gr}^k(r) - Q_{gr}^k(r) \tag{34}$$

$$\int_{r_k - \frac{\Delta r}{2}}^{r_k + \frac{\Delta r}{2}} R_{gr}^k(r) P_i^k(r) r dr = 0, \quad i = 0, 1, 2 \tag{35}$$

- Zeroth moment

$$\begin{aligned} &\frac{J_{gr+}^m(r_m + \frac{\Delta r_m}{2}) - J_{gr-}^m(r_m - \frac{\Delta r_m}{2})}{r_m \Delta r_m} + \\ &+ \Sigma_{t,g}^m \bar{\phi}_{gr}^m - \bar{Q}_{gr}^m = 0 \end{aligned} \tag{36}$$

$$\begin{aligned} &a_{g1}^m \frac{6\beta_g^m}{r_m} + a_{g2}^m \frac{24\beta_g^m}{\Delta r_m} - a_{g3}^m \frac{16\beta_g^m}{5r_m} + a_{g4}^m \frac{32\beta_g^m}{\Delta r_m} = \\ &= \Sigma_{t,g}^m \bar{\phi}_{gr}^m - \bar{Q}_{gr}^m \end{aligned} \tag{37}$$

- First moment

$$\varepsilon_{g1}^m = \frac{175\Delta r_m (12D_g^m + (12r_m^2 - \Delta r_m^2)\Sigma_{t,g}^m)}{r_m} \tag{38}$$

$$\varepsilon_{g2}^m = 280(-30D_g^m + \Delta r_m^2 \Sigma_{t,g}^m) \tag{39}$$

$$\begin{aligned} \varepsilon_{g3}^m = &\frac{1680D_g^m (10r_m^2 - \Delta r_m^2)}{r_m \Delta r_m} - \\ &- \frac{14\Delta r_m (-20r_m^2 + \Delta r_m^2 \Sigma_{t,g}^m)}{\Delta r_m} \end{aligned} \tag{40}$$

$$\varepsilon_{g4}^m = -160(140D_g^m + \Delta r_m^2 \Sigma_{t,g}^m) \tag{41}$$

$$\begin{aligned} \varepsilon_{g0}^m = &\frac{(15q_{g1}^m + 2q_{g2}^m) r_m \Delta r_m}{5} - \\ &- \frac{4(4q_{g4}^m - 7q_{g2}^m)\Delta r_m^2}{70} - \frac{(25q_{g1}^m + 2q_{g3}^m)\Delta r_m^3}{100 r_m} \end{aligned} \tag{42}$$

$$a_{g1}^m \varepsilon_{g1}^m + a_{g2}^m \varepsilon_{g2}^m + a_{g3}^m \varepsilon_{g3}^m + a_{g4}^m \varepsilon_{g4}^m = \varepsilon_{g0}^m \tag{43}$$

- Second moment

$$\tau_{g1}^m = 35\Delta r_m^2 \Sigma_{t,g}^m \tag{44}$$

$$\tau_{g2}^m = 70 r_m \Delta r_m \Sigma_{t,g}^m \tag{45}$$

$$\tau_{g3}^m = 4(105D_g^m + \Delta r_m^2 \Sigma_{t,g}^m) \tag{46}$$

$$\tau_{g4}^m = -\frac{40 r_m (140D_g^m + \Delta r_m^2 \Sigma_{t,g}^m)}{\Delta r_m} \tag{47}$$

$$\begin{aligned} \tau_{g0}^m = &-10(7q_{g2}^m - 4q_{g4}^m) r_m \Delta r_m - \\ &- \Delta r_m^2 (35q_{g1}^m + 4q_{g3}^m) \end{aligned} \tag{48}$$

$$a_{g1}^m \tau_{g1}^m + a_{g2}^m \tau_{g2}^m + a_{g3}^m \tau_{g3}^m + a_{g4}^m \tau_{g4}^m = \tau_{g0}^m \tag{49}$$

2.10 Boundary surfaces

One-node NEM approach has been applied to the surfaces that are located at the boundary of reactor core volume, as they are shared only by one node. In that case there are only four coefficients that describe the neutron flux expansion, which can be derived by applying the first three moments of the Galerkin weighted residual method, and albedo boundary condition, that is based on the P1 partial-currents and neutron flux relationship.

- Albedo boundary condition

$$\phi^k_{gr+}\alpha^k = -D^k_g \frac{d\phi^k_{gr+}}{dr} \tag{50}$$

$$a^k_{g1}(6\beta^k_g + \alpha^k(3 - \frac{\Delta r_k}{2r_k})) + a^k_{g2}(2\alpha^k + 12\beta^k_g) + \\ + a^k_{g3}(\frac{2D^k_g}{5r_k} - 4\beta^k_g) + 16a^k_{g4}\beta^k_g = -\alpha^k \bar{\phi}^k_{gr+} \tag{51}$$

2.11 Singularity neighboring surfaces

Alternative two-node approach has been applied to the surfaces that are located next to the singularity at radius $r = 0$. After investigation of the zeroth moment equation it was found that applying it to the node containing the singularity, leads to significant error. Therefore, the zeroth moment for the node containing the singularity has been replaced by reflective boundary condition at the singularity (52), while all other equations are formulated as for inner surfaces.

- Reflective boundary condition

$$-D^L_g \frac{d\phi^L_{gr-}}{dr} = 0 \tag{52}$$

$$-15a^L_{g1} + 30a^L_{g2} + a^L_{g3}(\frac{\Delta r_L + 10r_L}{r_L}) + 40a^L_{g4} = 0 \tag{53}$$

3. Validation of the code

CYNUS code has been validated against a cylindricalized 3D IAEA LWR benchmark problem [5]. It is a two-group problem featuring octant azimuthal symmetry, which makes it possible to calculate a 45-degree cut of the reactor core with imposed reflective boundary conditions. The reactor volume has been discretized:

- Radially into 9 sections of 10, 20, 25, 20, 25, 20, 15, 15, and 25 cm,
- Axially into 19 identical 20 cm sections,
- Azimuthally into 5 sections of 0.0982, 0.24545, 0.24545, 0.0982, and 0.0982 radians.

Figures 1, 2, and 3 represent axially integrated power density distributions, and relative errors in the azimuthal-radial plane.

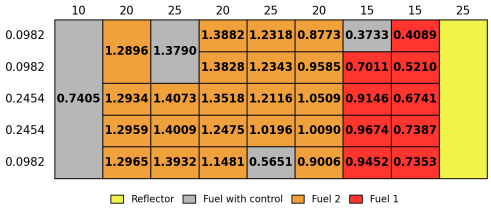


Fig. 1. Benchamrk reference normalized power density distribution.

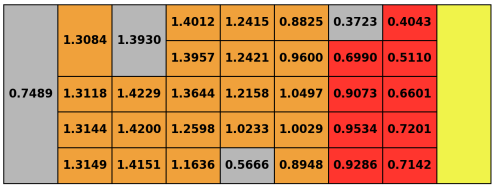


Fig. 2. Benchmark CYNUS normalized power density distribution.

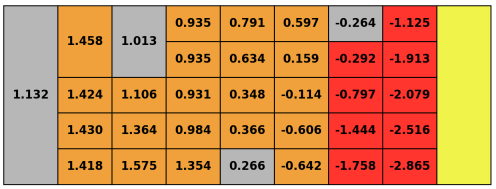


Fig. 3. Benchmark relative error between the CYNUS and reference power density distributions [%].

Table I: CYNUS validation against the 3D IAEA LWR benchmark.

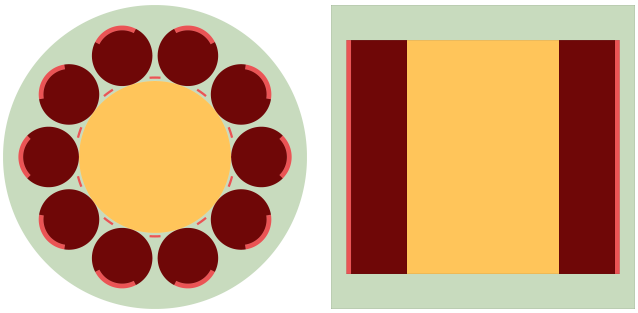
Parameter	Value	Unit
Reference k_{eff}	1.033530	[-]
CYNUS k_{eff}	1.033358	[-]
Δk_{eff}	-17.2	pcm
RMSE	0.9948	%

4. Multi-group MSR problem

After validation of the code, it has been applied to solve simplified Model-1 fast/thermal spectrum molten salt reactor conceptual design developed by FNC [9], problem in the cylindrical geometry, with multi-group structure of 33 energy groups. The reactor volume is filled with homogeneous fuel salt, and its reactivity is controlled by 10 rotating control drums and 10 withdrawable control plates. In considered problem all control plates are fully inserted and control drums are oriented away from the reactor core, which makes it azimuthally and axially symmetric. Therefore, a 18-degree and half axial height cut is enough to represent the entire reactor, by imposing appropriate reflective boundary conditions. Homogenized cross sections have been established via Serpent 2.2.1 for eight regions defined by the radial and axial cuts of the reactor core. The reactor volume has been discretized into:

- Radial cuts of 20, 30, 30 (reactor core) and 80cm (control drums and reflector),

- Axial cuts of 200 (reactor core) and 60cm (reflector).



(a) Top view. (b) Side view.

Fig. 4. Top and side view of the simplified Model-1 MSR core.

The reference solution has been obtained by applying a fine mesh to the problem and solving it by pure finite difference method. The CYNUS solution has been obtained using:

- Radial cuts of 2x 10, 4x 15, and 6x 13.33cm,
- Axial cuts of 13x 20cm,
- No azimuthal cuts.

Following figures represent solely the reactor core without the reflector and control elements in the axial-radial plane. Where bottom and left sides of a figures are assigned with the reflective boundary conditions.

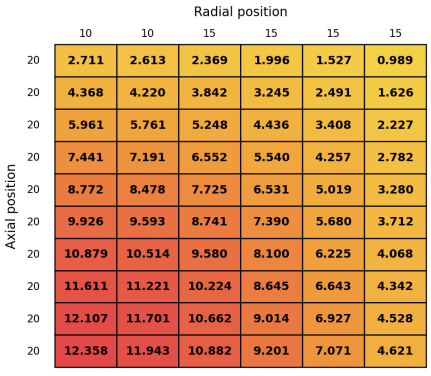


Fig. 5. MSR fine mesh FDM normalized power density distribution.

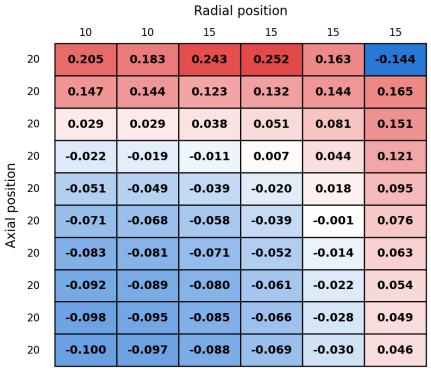


Fig. 6. MSR relative error between the CYNUS and reference power density distributions [%].

Table II: CYNUS MSR problem calculations result.

Parameter	Value	Unit
FMFD k_{eff}	0.939207	[-]
CYNUS k_{eff}	0.938997	[-]
Δk_{eff}	-21	pcm
RMSE	0.0969	%

5. Conclusion

A two-node CMFD formulation for cylindrical geometry, has been implemented in this work. By combining the Source Expansion Nodal Method for the azimuthal and axial directions with a Nodal Expansion Method for the radial direction, high accuracy with coarse mesh size has been achieved. Additionally, alternative approach has been proposed for the node containing the singularity at the center of cylindrical coordinate system for radial nodal routine. It has been shown that the zeroth moment of the Galerkin weighted residual method is not applicable for this node, and has been replaced by a reflective boundary condition. The code was validated against a cylindricalized IAEA 3D LWR benchmark and a multi-group fast/thermal spectrum MSR problem. In both cases, CYNUS reproduced the reference k_{eff} with high accuracy, yielding deviations of -17.2 pcm and -21 pcm, respectively, while the power density RMSE remained below 1% in both problems. In the MSR problem, RMSE was found to be 0.0969%, which may be attributed to the azimuthal symmetry of the problem, and multigroup structure where power density distribution is affected by all of the 33 energy groups. These results indicate that the proposed two-node kernel formulation, provides a numerically stable and computationally efficient alternative to already defined CMFD, analytical or fine-mesh FDM calculations for cylindrical reactor geometries.

Acknowledgement

This research was supported by the 2026 Research Fund of the KEPCO International Nuclear Graduate School (KINGS), the Republic of Korea.

References

[1] Bernard Ronald Bandini. A three-dimensional transient neutronics routine for the trac-pf1 reactor thermal hydraulic computer code. Technical report, Los Alamos National Laboratory (LANL), 5 1990.

[2] Nam Zin Cho and Jaejun Lee. Analytic function expansion nodal method for multigroup diffusion equations in cylindrical (r, θ, z) geometry. *Nuclear Science and Engineering*, 159:229–241, 7 2008.

[3] A M Ougouag and W K Terry. Development of a nodal method for the solution of the neutron diffusion equation in general cylindrical geometry. Technical report, 2002.

[4] Yutong Wen, Ding She, and Lei Shi. Improvement of cylindrical nodal expansion method for treating htgr void cavity. *Progress in Nuclear Energy*, 161:104714, 7 2023.

[5] Rian H. Prinsloo and Djordje I. Tomašević. The analytic nodal method in cylindrical geometry. *Nuclear Engineering and Design*, 238:2898–2907, 11 2008.

[6] Dengying Wang, Fu Li, Jiong Guo, Jinfeng Wei, Jingyu Zhang, and Chen Hao. Improved nodal expansion method for solving neutron diffusion equation in cylindrical geometry. *Nuclear Engineering and Design*, 240:1997–2004, 8 2010.

[7] Joo Il Yoon and Han Gyu Joo. Two-level coarse mesh finite difference formulation with multigroup source expansion nodal kernels. *Journal of Nuclear Science and Technology*, 45:668–682, 2008.

[8] O.G. Komlev and I.R. Suslov. *A nodal expansion method for the neutron diffusion equation in cylindrical geometry*. American Nuclear Society, Inc., 1995.

[9] Yubin Go, Tongkyu Park, Sung Kyun Zee, Jae Uk Seo, and Seong Jun Yoon. Conceptual core design study of a maritime molten salt fast reactor. *Annals of Nuclear Energy*, 222:111571, 11 2025.